

# Finite-Size Effects of Binary Mutual Diffusion Coefficients from Molecular Dynamics

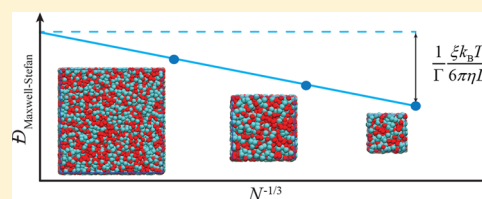
Seyed Hossein Jamali,<sup>†</sup> Ludger Wolff,<sup>‡</sup> Tim M. Becker,<sup>†</sup> André Bardow,<sup>‡</sup> Thijs J. H. Vlugt,<sup>†</sup> and Othonas A. Moulton<sup>\*,†</sup>

<sup>†</sup>Engineering Thermodynamics, Process & Energy Department, Faculty of Mechanical, Maritime and Materials Engineering, Delft University of Technology, Leeghwaterstraat 39, 2628CB Delft, The Netherlands

<sup>‡</sup>Institute of Technical Thermodynamics, RWTH Aachen University, 52056 Aachen, Germany

## S Supporting Information

**ABSTRACT:** Molecular dynamics simulations were performed for the prediction of the finite-size effects of Maxwell–Stefan diffusion coefficients of molecular mixtures and a wide variety of binary Lennard–Jones systems. A strong dependency of computed diffusivities on the system size was observed. Computed diffusivities were found to increase with the number of molecules. We propose a correction for the extrapolation of Maxwell–Stefan diffusion coefficients to the thermodynamic limit, based on the study by Yeh and Hummer (*J. Phys. Chem. B*, 2004, 108, 15873–15879). The proposed correction is a function of the viscosity of the system, the size of the simulation box, and the thermodynamic factor, which is a measure for the nonideality of the mixture. Verification is carried out for more than 200 distinct binary Lennard–Jones systems, as well as 9 binary systems of methanol, water, ethanol, acetone, methylamine, and carbon tetrachloride. Significant deviations between finite-size Maxwell–Stefan diffusivities and the corresponding diffusivities at the thermodynamic limit were found for mixtures close to demixing. In these cases, the finite-size correction can be even larger than the simulated (finite-size) Maxwell–Stefan diffusivity. Our results show that considering these finite-size effects is crucial and that the suggested correction allows for reliable computations.



## 1. INTRODUCTION

The knowledge of diffusion in liquid mixtures is essential for the design and optimization of various industrial processes.<sup>1–9</sup> Although experimental methods are constantly improving,<sup>10–16</sup> measurements of diffusion coefficients for multicomponent systems are not always feasible or straightforward to perform. Diffusion experiments may require specialized equipment and materials and they can be very time-consuming and expensive.<sup>11,17</sup> For these reasons, semiempirical models such as the Stokes–Einstein,<sup>18</sup> Chapman–Enskog,<sup>19</sup> and Wilke–Chang<sup>20</sup> models have been developed for predicting diffusion coefficients.<sup>21–27</sup> However, the applicability of these models is usually limited to gases or infinitely dilute mixtures.

In this context, molecular dynamics (MD) simulations are a powerful tool to complement or even, in some cases, substitute experiments for computing diffusion coefficients.<sup>28–41</sup> In MD simulations, the trajectories of molecules in a simulation box are obtained by integrating Newton’s second law. Conventional MD simulations yield Maxwell–Stefan (MS) diffusion coefficients, from which Fick diffusivities can be calculated using the so-called thermodynamic factor.<sup>6–8,42–44</sup>

One of the advantages of MD is that these simulations are not limited to diffusion in bulk fluids but can also be employed for more complex systems like the diffusion of gases/liquids in porous membranes.<sup>45–50</sup> Due to the intrinsic inclusion of the nonideal behavior of mixtures, MD simulations have the potential to foster the deep understanding of diffusion

phenomena<sup>51–53</sup> and verify empirical correlations for predicting diffusivities.<sup>54–58</sup> It is important to note that, even with modern computers, the number of molecules considered in a typical MD simulation is orders of magnitude lower than the thermodynamic limit. Thus, it is important to take into account finite-size effects when calculating diffusion coefficients. Previously, simulations of thermodynamic and transport properties for systems close to critical points<sup>59–61</sup> and phase transitions<sup>62–64</sup> have also shown that corrections for the finite size effects should be applied.

It has been shown that self-diffusivities computed from MD simulations scale linearly with  $N^{-1/3}$ , where  $N$  is the number of molecules in the simulation box.<sup>65</sup> Yeh and Hummer<sup>66</sup> performed a detailed investigation of this behavior for Lennard–Jones (LJ) particles and water molecules. The authors found that the finite-size effects originate from hydrodynamics and derived a correction term. By adding this term to the computed self-diffusivity by MD simulation, the self-diffusivity in the thermodynamic limit can be accurately determined. Several studies verified the applicability of the YH correction for systems of nonspherical molecules.<sup>67–69</sup> According to Yeh and Hummer,<sup>66</sup> the system size effects of the diffusivity of charged molecules in a polar or ionic medium cannot be accurately corrected with the proposed term. These

Received: February 15, 2018

Published: April 17, 2018

deviations are due to the strong electrostatic interactions, and thus, the correction term needs rescaling.

To the best of our knowledge, no study has focused on the finite-size effects of MS or Fick diffusivities and noninfinitely diluted mixtures, obtained from MD simulations. In this study, we show that, depending on the size of the system, there can be significant differences between the simulated (finite size) and real (thermodynamic limit) MS diffusion coefficients in binary mixtures. For systems close to demixing, the finite-size correction can be even larger than the simulated diffusivity. For self-diffusion, the finite-size effects depend only on the box size, temperature, and viscosity, but for MS diffusivity, there is also a strong dependence on the nonideality of the mixture (represented by the thermodynamic factor). We propose a finite-size correction for MS diffusion and verify its accuracy for a large number of LJ and molecular mixtures.

This paper is organized in five sections. In Section 2, theoretical aspects of self and MS diffusion are briefly discussed. In Section 3, details of the MD simulations and the studied mixtures are explained. A detailed analysis of the results of the MD simulations and the proposed correction term to finite-size mutual diffusivities is provided in Section 4. Finally, the conclusions of this study are summarized.

## 2. THEORY

There are two approaches for obtaining transport properties from MD simulations: (a) nonequilibrium molecular dynamics (NEMD), which employ an external driving force generating a net flux in the system,<sup>28,70–77</sup> and (b) equilibrium molecular dynamics (EMD), where transport coefficients are computed from time-correlation functions in a system at equilibrium, without the presence of external forces.<sup>9,75,77,78</sup> In this work, we perform only EMD simulations. Sampling time correlations can be achieved via two formulations, which are intrinsically identical: Einstein and Green–Kubo.<sup>75,77,78</sup> The Einstein formulation is used in this work. For an overview of EMD and NEMD methods, the reader is referred to the reviews by Liu et al.<sup>9</sup> and Peters et al.<sup>11</sup>

The following three types of diffusion coefficients are discussed in this manuscript: (1) the self-diffusion coefficient ( $D_{\text{self}}$ ), which is the diffusivity of a tagged particle in a medium due to its Brownian motion; (2) the Fick diffusivity ( $D_{\text{Fick}}$ ), which is the coefficient of the linear relation between the mass flux and the concentration gradient in the system; (3) the MS diffusivity ( $D_{\text{MS}}$ ), which describes mass transport due to the gradient in chemical potential of a species in a mixture.  $D_{\text{self}}$  has to do with the motion of individual molecules, while  $D_{\text{Fick}}$  and  $D_{\text{MS}}$  are due to the collective motion of all molecules in the system. Hence, for  $D_{\text{Fick}}$  and  $D_{\text{MS}}$ , the term “collective” or “mutual” diffusion is used. Although the MS diffusivity provides a more general description of transport diffusion in multi-component mixtures,<sup>42</sup> the Fick diffusivity is widely used in industry due to its simplicity. For homogeneous mixtures, the Fick and MS diffusion coefficients are related by the so-called thermodynamic factor ( $\Gamma$ ), which is related to the nonideality of the system.<sup>79,80</sup> An extensive analysis and comparison of Fick and MS diffusion coefficients can be found in literature.<sup>42–44</sup> A more detailed description of these three types of diffusion coefficients is provided in the following two subsections.

**2.1. Self-Diffusion Coefficients.** The self-diffusion coefficient of species  $i$  ( $D_{i,\text{self}}$ ) can be expressed as the mean-square displacement of each molecule of species  $i$ :

$$D_{i,\text{self}} = \lim_{t \rightarrow \infty} \frac{1}{6N_i t} \left\langle \sum_{j=1}^{N_i} (\mathbf{r}_{j,i}(t) - \mathbf{r}_{j,i}(0))^2 \right\rangle \quad (1)$$

where  $t$  is the correlation time,  $N_i$  is the number of molecules of species  $i$ , and  $\mathbf{r}_{j,i}$  is the position of  $j$ -th molecule of species  $i$ . The angle brackets denote an ensemble average. Self-diffusion coefficients computed from MD simulations depend strongly on the number of molecules,  $N$ , in the simulation box. More specifically, it was shown that self-diffusivity scales linearly with  $1/N^{1/3}$ , which is equivalent to  $1/L$ , where  $L$  is the side length of the simulation box.<sup>65</sup> Yeh and Hummer<sup>66</sup> studied the size dependency of computed self-diffusion coefficients and derived an analytic correction term to compensate for the observed system-size effects. The correction term was developed on the basis of the hydrodynamic theory for a spherical particle in a Stokes flow with imposed periodic boundary conditions. These authors showed that the difference between the self-diffusivity in an infinite (nonperiodic) and a finite (periodic) system is due to the difference in hydrodynamic self-interactions.<sup>65,81</sup> For the rest of this manuscript, we will refer to their correction term as the “YH correction”. Accordingly, the self-diffusion coefficient of species  $i$  in the thermodynamic limit ( $D_{i,\text{self}}^\infty$ ) can be estimated from the finite-size self-diffusion coefficient obtained from MD simulations ( $D_{i,\text{self}}^{\text{MD}}$ ) by adding the YH correction ( $D^{\text{YH}}$ ):<sup>66</sup>

$$D_{i,\text{self}}^\infty = D_{i,\text{self}}^{\text{MD}} + D^{\text{YH}}(T, \eta, L) = D_{i,\text{self}}^{\text{MD}} + \frac{\xi k_B T}{6\pi\eta L} \quad (2)$$

where  $k_B$  is the Boltzmann constant,  $L$  is the side length of the simulation box, and  $\eta$  is the shear viscosity of the system at temperature  $T$ .  $\xi$  is a dimensionless constant equal to 2.837297 for cubic simulation boxes with periodic boundary conditions.<sup>66</sup> Similar to the YH correction, equations have been derived for simulations in noncubic boxes<sup>82–84</sup> and for confined fluids.<sup>85</sup> It is important to note that the YH correction does not explicitly depend on the size of molecules in a fluid or intermolecular interactions. This means that all species of a multicomponent mixture experience identical finite-size effects.

In EMD simulations, the required shear viscosity can be computed from the autocorrelation of the off-diagonal components of the stress tensor ( $P_{\alpha\beta}$ ):<sup>77,78,86,87</sup>

$$\eta = \lim_{t \rightarrow \infty} \frac{1}{2t} \frac{V}{k_B T} \left\langle \left( \int_0^t P_{\alpha\beta}(t') dt' \right)^2 \right\rangle \quad (3)$$

where  $V$  is the volume of the system. The components of the stress tensor are composed of two parts: an ideal and a virial term. The first part is due to the total kinetic energy of particles, and the second is constructed from intra- and intermolecular interactions.<sup>77,88,89</sup> The three off-diagonal components of the stress tensor ( $P_{xy}$ ,  $P_{xz}$ , and  $P_{yz}$ ) yield three values for the shear viscosity, which are equal for isotropic fluids. As shown in the work of Yeh and Hummer<sup>66</sup> and Moulton et al.<sup>69</sup> as well as in the current study (Supporting Information), the shear viscosity is independent of the system size. Therefore, the viscosity is a constant in eq 2.

**2.2. Maxwell–Stefan and Fick Diffusion Coefficients.** MS diffusion coefficients can be obtained from the Onsager coefficients ( $\Lambda_{ij}$ ), computed from the crosscorrelation of the displacement of the molecules of species  $i$  and  $j$ :<sup>5–7,9,32,54</sup>

$$\Lambda_{ij} = \lim_{t \rightarrow \infty} \frac{1}{6Nt} \left\langle \left( \sum_{k=1}^{N_i} (r_{k,i}(t) - r_{k,i}(0)) \right) \times \left( \sum_{l=1}^{N_j} (r_{l,j}(t) - r_{l,j}(0)) \right) \right\rangle \quad (4)$$

where  $N_i$  and  $N_j$  are the number of molecules of species  $i$  and  $j$ , respectively, and  $N$  is the total number of molecules in the mixture.  $r_{l,j}$  is the position of the  $l$ -th molecule of species  $j$ . The Onsager coefficients ( $\Lambda_{ij}$ ) in eq 4 are defined in a reference frame in which the velocity of the center of mass is zero.<sup>32</sup> Hence, the Onsager coefficients of a binary mixture are correlated by means of the molar masses of the two constituent species ( $M_1$  and  $M_2$ ):<sup>32</sup>

$$\Lambda_{12} = -\left(\frac{M_1}{M_2}\right)\Lambda_{11} = -\left(\frac{M_2}{M_1}\right)\Lambda_{22} \quad (5)$$

The Onsager coefficient of species  $i$  ( $\Lambda_{ii}$ ) can be split into an autocorrelation term, which is the self-diffusivity of species  $i$  ( $D_{i,\text{self}}$ ), and a crosscorrelation term ( $CC_{ii}$ ):<sup>6,51</sup>

$$\Lambda_{ii} = \lim_{t \rightarrow \infty} \frac{1}{6Nt} \left\langle \left( \sum_{k=1}^{N_i} (r_{k,i}(t) - r_{k,i}(0))^2 \right) \right\rangle + \lim_{t \rightarrow \infty} \frac{1}{6Nt} \left\langle \left( \sum_{k=1}^{N_i} (r_{k,i}(t) - r_{k,i}(0)) \right) \times \left( \sum_{l=1, l \neq k}^{N_i} (r_{l,i}(t) - r_{l,i}(0)) \right) \right\rangle = x_i D_{i,\text{self}} + CC_{ii} \quad (6)$$

The Onsager coefficient of two different species ( $\Lambda_{ij}$ , where  $i \neq j$ ) is a displacement crosscorrelation of the constituent two species:

$$\Lambda_{ij, i \neq j} = CC_{ij} \quad (7)$$

The MS diffusion coefficient of a binary system is a linear combination of the Onsager coefficients. These relations for binary, ternary, and quaternary mixtures are listed in the articles by Krishna and van Baten<sup>32</sup> and Liu et al.<sup>54</sup> For a binary mixture with mole fractions of  $x_1$  and  $x_2$ , a single MS diffusion coefficient is defined ( $D_{12,MS} = D_{21,MS} = D_{MS}$ ):<sup>32</sup>

$$D_{MS} = \frac{x_2}{x_1} \Lambda_{11} + \frac{x_1}{x_2} \Lambda_{22} - 2\Lambda_{12} \quad (8)$$

Using the constraint of eq 5, eq 8 can be rewritten as separate functions of the Onsager coefficients:

$$\begin{aligned} D_{MS} &= -\left[ \frac{(M_2 + x_1(M_1 - M_2))^2}{x_1 x_2 M_1 M_2} \right] \Lambda_{12} \\ &= +\left[ \frac{(M_2 + x_1(M_1 - M_2))^2}{x_1 x_2 M_2^2} \right] \Lambda_{11} \\ &= +\left[ \frac{(M_2 + x_1(M_1 - M_2))^2}{x_1 x_2 M_1^2} \right] \Lambda_{22} \end{aligned} \quad (9)$$

Equations 8 and 9 are valid for both ideal and nonideal diffusing binary mixtures. For ideal diffusing mixtures, the crosscorrelation between the particles is rather small compared to the self-diffusivities, which means that in eqs 6–8 ( $x_2/x_1$ )  $CC_{11} + (x_1/x_2)CC_{22} - 2CC_{12} \ll x_2 D_{1,\text{self}} + x_1 D_{2,\text{self}}$  and therefore, the MS diffusivity (eq 8) can be simplified to the Darken equation ( $D_{\text{Darken}}$ ):<sup>6,51,54</sup>

$$D_{\text{Darken}} = x_2 D_{1,\text{self}} + x_1 D_{2,\text{self}} \quad (10)$$

Converting MS to Fick diffusivities requires the so-called thermodynamic factor  $\Gamma$ :<sup>7,42,79</sup>

$$D_{\text{Fick}} = \Gamma D_{\text{MS}} = \left[ 1 + \frac{\partial \ln \gamma_1}{\partial \ln x_1} \right]_{T,p} D_{\text{MS}} \quad (11)$$

where  $\Gamma$  is the thermodynamic factor of a binary mixture and  $\gamma_1$  is the activity coefficient of species 1. For an  $n$ -component mixture, the thermodynamic factor is defined as a matrix whose elements are<sup>43</sup>

$$\Gamma_{ij} = \delta_{ij} + \frac{\partial \ln \gamma_i}{\partial \ln x_j} \Big|_{T,p,\Sigma} \quad (12)$$

where  $\delta_{ij}$  is the Kronecker delta.  $\Sigma$  indicates that the derivative is taken at constant mole fractions of all species, except for the  $n^{\text{th}}$  species.<sup>43</sup>

A stable single-phase binary mixture requires that  $\Gamma > 0$ .<sup>79,80</sup> For ideal mixtures,  $\Gamma = 1$  by definition. Binary mixtures with a thermodynamic factor between 0 and 1 favor interactions between the same species over interactions between different species. Systems with a thermodynamic factor larger than one exhibit associating behavior.<sup>28,43</sup> Thermodynamic factors can be calculated with equations of state,<sup>32,42</sup> Kirkwood–Buff integrals,<sup>9,90–92</sup> or the permuted Widom test particle insertion method.<sup>93,94</sup> In this study, the thermodynamic factors for binary systems are obtained from finite-size Kirkwood–Buff coefficients. The finite-size Kirkwood–Buff integral equals:<sup>9</sup>

$$\begin{aligned} G_{ij}^V &= \frac{1}{V} \int_V \int_V (g_{ij}(r) - 1) d\mathbf{r}_1 d\mathbf{r}_2 \\ &= 4\pi \int_0^{2R} [g_{ij}(r) - 1] \left[ 1 - \frac{3r}{4R} + \frac{r^3}{16R^3} \right] r^2 dr \end{aligned} \quad (13)$$

where  $g_{ij}(r)$  is the radial distribution function,  $r = |r_1 - r_2|$ , and the integration is over a finite spherical subvolume  $V$  with radius  $R$ . As  $G_{ij}^V$  scales linearly with  $1/R$ , the Kirkwood–Buff coefficient in the thermodynamic limit can be obtained by extrapolating the linear regime to  $1/R \rightarrow 0$ .<sup>95</sup> It is important to note that one needs to correct for finite-size effects of the radial distribution function. This correction is performed using the procedure outlined by Ganguly and van der Vegt<sup>96</sup> and Milzetti et al.,<sup>97</sup> For a binary system, the thermodynamic factor follows from

$$\Gamma = \frac{1}{1 + c_r x_1 x_2 (G_{11} + G_{22} - 2G_{12})} \quad (14)$$

Similar expressions exist for ternary and multicomponent systems.<sup>91,92</sup>

### 3. SIMULATION DETAILS

All simulations in this study were performed in cubic simulation boxes. Periodic boundary conditions were imposed in all directions. All MD simulations were conducted with LAMMPS<sup>98</sup> (version 16 Feb. 2016). The initial configurations and LAMMPS input files were constructed with PACKMOL<sup>99</sup> and VMD.<sup>100</sup>

To study the finite-size effects of MS diffusion coefficients in binary mixtures, two sets of MD simulations were carried out. The first set consists of binary LJ systems. All parameters and properties of these simulations are reported in dimensionless

units with the  $\epsilon$  and  $\sigma$  parameters of the first species as the base units:  $\sigma_1 = \sigma = 1$ ,  $\epsilon_1 = \epsilon = 1$ , and mass =  $m_1 = m = 1$ . The characteristics of the second species ( $\epsilon_2$ ,  $\sigma_2$ , and  $m_2 = \sigma_2^3$ ), mole fractions ( $x$ ), and adjustable parameters ( $k_{ij}$ ) of all studied LJ systems are listed in Table 1. The applied temperature  $T$  and

**Table 1. Specifications of the Studied LJ Systems<sup>a</sup>**

specification	values
total number of particles	500, 1000, 2000, 4000
independent simulations	10, 10, 5, 5
$x_1$	0.1, 0.3, 0.5, 0.7, 0.9
$\epsilon_2/\epsilon_1$	1.0, 0.8, 0.6, 0.5
$\sigma_2/\sigma_1$	1.0, 1.2, 1.4, 1.6
$m_2/m_1$	$(\sigma_2/\sigma_1)^3$
$k_{ij}$	0.05, 0.0, -0.3, -0.6

<sup>a</sup>LJ particle type 1 has  $\sigma_1 = \sigma = 1.0$ ,  $\epsilon_1 = \epsilon = 1.0$ , and mass =  $m_1 = 1.0$  in dimensionless units.<sup>77</sup> As explained in the Supporting Information (eq. S3),  $k_{ij}$  is an adjustable parameter to the Lorentz–Berthelot mixing rules, controlling the nonideality in the mixtures.

pressure  $p$  in the simulations are 0.65 and 0.05, respectively. The number density of the studied systems is between 0.14 and 0.89. A time step of 0.001 is used for the integration of equations of motion. Displacement and stress correlation functions are computed for a total length of 200 million time steps. In total, 320 distinct LJ systems with four system sizes (500, 1000, 2000, and 4000 particles) are simulated. To create a sound data set, systems in which phase separation occurs or a considerable deviation of the pressure or temperature from the specified conditions is observed are excluded from the data analysis. These systems correspond to a small fraction of the total data set. The second set of MD simulations includes 9 binary mixtures consisting of molecular systems. An overview of these mixtures, consisting of methanol as the first component and water, ethanol, acetone, methylamine, or carbon tetrachloride as the second component, is listed in Table 2. For each

**Table 2. Specifications of All Studied Binary Molecular Systems<sup>a</sup>**

specification	values
total number of molecules	250, 500, 1000, 2000
independent simulations	10, 10, 10, 10
second component (mole fraction)	water (0.1, 0.3, 0.5, 0.7, 0.9) ethanol (0.5) acetone (0.5) methylamine (0.5) carbon tetrachloride (0.1)

<sup>a</sup>The first component for all mixtures is methanol. The mole fraction of the second component is specified in parentheses. The force field parameters are available in the Supporting Information.

mixture, four system sizes (250, 500, 1000, and 2000 molecules) are considered. The temperature and pressure are specified to be 298 K and 1.0 atm. The total length of each simulation is 200 ns with an integration time step of 1 fs.

The force fields used in this work for both LJ and molecular systems are explained in detail in the Supporting Information. For the LJ systems, interactions are truncated and shifted to zero at a cutoff radius of  $4\sigma$ .<sup>77</sup> The Lorentz–Berthelot mixing rules with an adjustment parameter ( $k_{ij}$ ), controlling the nonideality of mixtures, are applied to the LJ parameters of

dissimilar particles.<sup>77</sup> For the molecular systems, the SPC/E model<sup>101</sup> and the model proposed by Tummala and Striolo<sup>102</sup> are used for water and carbon tetrachloride molecules, respectively. The force field parameters for methanol,<sup>103</sup> ethanol,<sup>103</sup> acetone,<sup>104</sup> and methylamine<sup>105,106</sup> are obtained from the Transferable Potential for Phase Equilibria (TraPPE) force field.<sup>106</sup> The LJ interactions are truncated at 10.0 Å, and analytic tail corrections for energy and pressure are included.<sup>77</sup> The Lorentz–Berthelot mixing rules for dissimilar interaction sites are applied.<sup>77</sup> Long-range electrostatic interactions are taken into account by means of the particle–particle–particle–mesh (PPPM) method with a relative precision of  $10^{-6}$ .<sup>77</sup> It is important to note that the aim of this study is not to compare computed transport properties with experiments but to study finite-size effects observed in mutual diffusion coefficients. We adopt these well-known force fields, which have already been used by many researchers for computing transport properties.<sup>6–8,55,69,107–109</sup>

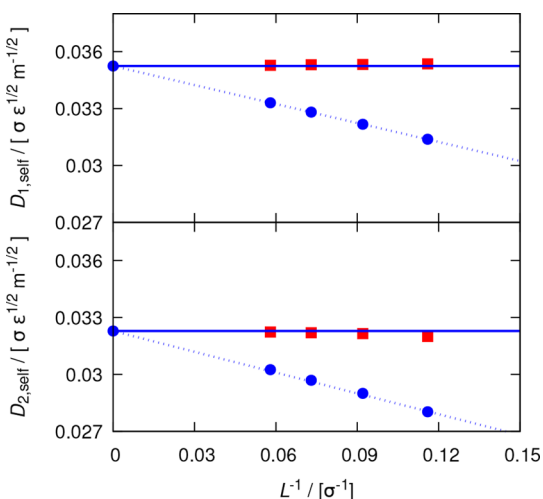
For both data sets and each data point, at least five independent simulations were carried out to obtain the average properties and their 95% confidence intervals. For better sampling of displacement and stress correlation functions, the order- $n$  algorithm was used.<sup>75,110</sup> As explained in the previous section, the thermodynamic factors were calculated from the RDFs of the constituent species using finite-size Kirkwood–Buff integrals.<sup>92</sup> The RDFs were computed from MD simulations of large systems in the canonical ensemble. These systems contain 25 000 LJ particles (first set of simulations) and 13 500 molecules (second set of simulations). The total length of simulations for computing the Kirkwood–Buff integrals is 10 million time steps for the LJ systems and 10 ns for the molecular mixtures.

## 4. RESULTS AND DISCUSSIONS

We performed two sets of simulations. The first set consists of 250 distinct binary LJ systems, and the second set includes 9 binary mixtures consisting of methanol, water, ethanol, acetone, methylamine, and carbon tetrachloride. For each set, four system sizes were considered (Tables 1 and 2). All raw data for diffusion coefficients, shear viscosities, and thermodynamic factors is provided in the Supporting Information.

Previous studies on the system-size dependencies of self-diffusion coefficients are limited to pure fluids and infinitely diluted mixtures. Figure 1 shows an example of the self-diffusivities of the two components of a binary LJ systems as a function of the length of the simulation box ( $L$ ). Like in pure fluids, the computed self-diffusion coefficients vary linearly with the inverse of the simulation box length. The linear regression at  $1/L = 0$  yields the self-diffusivity for an infinite system size ( $D_{i,\text{self}}^\infty$ ), which is shown in the same figure as a horizontal line. The finite-size self-diffusivities corrected with  $D^{\text{YH}}$  (Equation 2) are plotted as red squares. As expected, the corrected self-diffusivities collapse on the horizontal line, indicating the validity of YH correction.

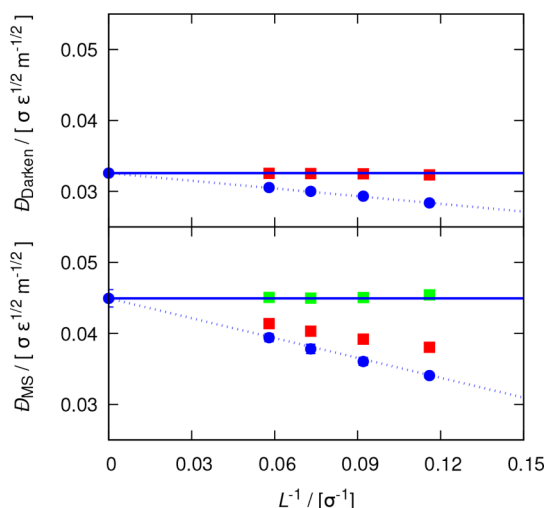
In Figure 2, the differences between the infinite and finite-size self-diffusivities ( $D_{i,\text{self}}^\infty - D_{i,\text{self}}^{\text{MD}}$ ) are plotted as a function of the YH correction ( $D^{\text{YH}}$ ), for all entries in the data set examined. For the majority of the cases, the YH correction term is able to predict the finite-size discrepancies very accurately. However, while the correction is almost perfect for molecular mixtures, a systematic overprediction of self-diffusivities can be observed for LJ systems. This overprediction becomes more pronounced as the difference between the size and the



**Figure 1.** Self-diffusion coefficients of a binary LJ mixture ( $x_1 = 0.9$ ) as a function of the simulation box length ( $L$ ). Blue circles are the computed self-diffusion coefficients in the finite systems, and red squares are the corrected values using the YH correction term (eq 2). The dashed lines indicate extrapolation to the thermodynamic limit, and the solid lines show the extrapolated self-diffusivities. The second component has  $\epsilon_2 = 0.5 \times \epsilon_1$  and  $\sigma_2 = 1.2 \times \sigma_1$ , and the adjustable parameter ( $k_{ij}$ ) to the Lorentz–Berthelot mixing rules is 0. The error bars are smaller than the symbols.

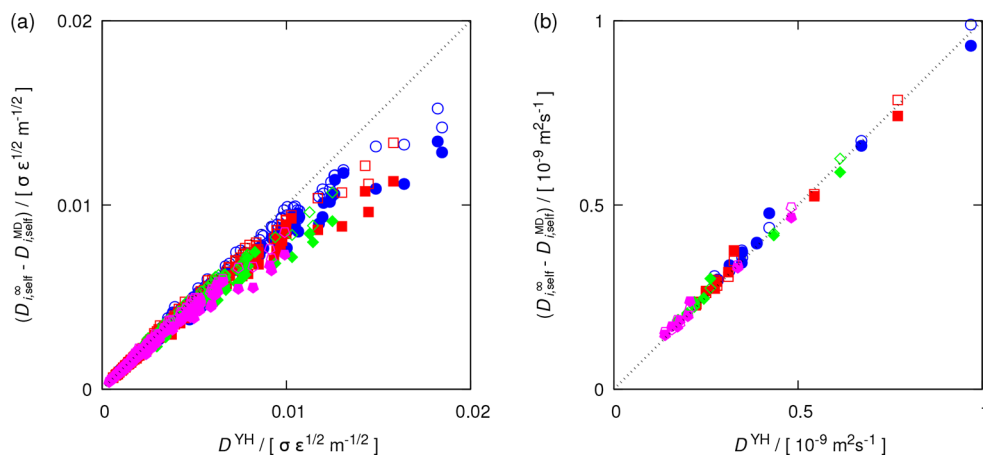
interaction energies of the species in the system increases. Out of the 250 LJ systems considered, 13 correspond to systems containing particles with large dissimilarities in size ( $\sigma_2/\sigma_1$  equal to 1.6 and 1.4) and interaction energy ( $\epsilon_2/\epsilon_1$  equal to 0.5 and 0.6). This finding indicates that, although the YH correction can be safely applied to binary systems with a wide variety of composition, nonideality, and relative size of particles, limitations exist for mixtures with significant differences between the size of the molecules and interaction energies.

Figure 3 illustrates the finite-size effects of the Darken equation ( $\mathcal{D}_{\text{Darken}}$ , eq 10) and MS diffusivities ( $\mathcal{D}_{\text{MS}}$ , eq 8) for the same binary LJ mixture of Figure 1. In the top figure, it is shown that the application of the YH correction,  $D^{\text{YH}}$ , to the



**Figure 3.** Diffusion coefficients of a binary LJ mixture ( $x_1 = 0.9$ ) as a function of the simulation box length ( $L$ ). Blue circles are the computed Darken (eq 10) and MS (eq 8) diffusivities. Red and green squares are the corrected values according to the YH (eq 2) and the MSYH (eq 17), respectively. The dashed lines show extrapolation to the thermodynamic limit, and the solid lines show the extrapolated values. The second component has  $\epsilon_2 = 0.5 \times \epsilon_1$  and  $\sigma_2 = 1.2 \times \sigma_1$ , and the adjustment parameter ( $k_{ij}$ ) to the Lorentz–Berthelot mixing rules is 0. The error bars are smaller than the symbols.

self-diffusivities of species 1 and 2 to the Darken equation (Equation 10) accurately accounts for the finite-size effects of  $\mathcal{D}_{\text{Darken}}$ . In the bottom figure, the application of the same corrections to MS diffusion coefficients is shown. The corrected  $\mathcal{D}_{\text{MS}}$  (red squares) are systematically lower than the extrapolated MS diffusivity, indicating that  $D^{\text{YH}}$  is not a valid correction for the finite effects of  $\mathcal{D}_{\text{MS}}$ . To further investigate this, the finite-size effect of the MS diffusivity can be obtained from eq 6 and 9 as follows:



**Figure 2.** Finite-size corrections required for self-diffusion coefficients as a function of the YH correction ( $D^{\text{YH}}$ , Equation 2) for (a) LJ and (b) molecular mixtures computed with 500 LJ particles/250 molecules (blue circles), 1000 LJ particles/500 molecules (red squares), 2000 LJ particles/1000 molecules (green diamonds), and 4000 LJ particles/2000 molecules (magenta pentagons). Closed and open symbols represent the corrections to the self-diffusivity of species 1 and species 2, respectively. The dashed lines indicate perfect agreement. Statistical uncertainties are listed in the Supporting Information.

$$\begin{aligned}
 \mathcal{D}_{\text{MS}}^{\infty} - \mathcal{D}_{\text{MS}}^{\text{MD}} &= \left[ \frac{(M_2 + x_1(M_1 - M_2))^2}{x_1 x_2} \right] \frac{1}{M_2^2} (\Lambda_{11}^{\infty} - \Lambda_{11}^{\text{MD}}) \\
 &= \frac{\alpha'}{M_2^2} [(x_1 D_{1,\text{self}}^{\infty} + CC_{11}^{\infty}) - (x_1 D_{1,\text{self}}^{\text{MD}} + CC_{11}^{\text{MD}})] \\
 &= \frac{\alpha'}{M_2^2} [x_1 (D_{1,\text{self}}^{\infty} - D_{1,\text{self}}^{\text{MD}}) + (CC_{11}^{\infty} - CC_{11}^{\text{MD}})] \\
 &= \frac{\alpha'}{M_2^2} [x_1 D^{\text{YH}} + (CC_{11}^{\infty} - CC_{11}^{\text{MD}})] \\
 &= \frac{\alpha'}{M_1^2} [x_2 D^{\text{YH}} + (CC_{22}^{\infty} - CC_{22}^{\text{MD}})] \quad (15)
 \end{aligned}$$

where  $\alpha'$  is a constant, which is unknown at this point.  $\mathcal{D}_{\text{MS}}^{\infty}$  and  $\mathcal{D}_{\text{MS}}^{\text{MD}}$  are the MS diffusivities in the thermodynamic limit and finite-size systems, respectively.  $CC_{ii}^{\infty}$  and  $CC_{ii}^{\text{MD}}$  are the infinite and finite-size displacement crosscorrelation functions of species  $i$ . As shown in Figure 3, in nonideal mixtures, the total displacement crosscorrelation function of all particles has a considerable contribution to the finite-size effect. At this point, we hypothesize that a modified YH correction term can be applied directly to the MS diffusion coefficients. Thus, the crosscorrelation terms of eq 15,  $CC_{ii}^{\infty} - CC_{ii}^{\text{MD}}$ , can be a function or simply a modification factor of the YH correction. Since the crosscorrelation terms are directly related to the nonideality of a mixture, it is expected that this modification factor is a function of the thermodynamic factor ( $\Gamma$ ):

$$\begin{aligned}
 \mathcal{D}_{\text{MS}}^{\infty} - \mathcal{D}_{\text{MS}}^{\text{MD}} &= \frac{\alpha'}{M_1^2} [x_2 D^{\text{YH}} + (CC_{22}^{\infty} - CC_{22}^{\text{MD}})] \\
 &= \frac{\alpha'}{M_1^2} [x_2 D^{\text{YH}} + \alpha'' D^{\text{YH}}] \\
 &= \alpha(\Gamma) \times D^{\text{YH}} \quad (16)
 \end{aligned}$$

where  $\alpha(\Gamma)$  is the modification factor to the YH correction, accounting for the finite-size effects of the MS diffusion coefficient. In the example shown in Figure 3, the thermodynamic factor of the mixture,  $\Gamma$ , is 0.35 and the modification factor required to scale the YH correction from the red squares to the green squares is roughly 3, which is approximately equal to  $1/\Gamma$ . To examine if  $1/\Gamma$  is a suitable modification of the YH correction for correcting the finite-size effect of MS diffusion coefficients, a phenomenological approach is followed: In Figure 4,  $1/\Gamma$  is compared to the required modification factor to  $D^{\text{YH}}$  for all LJ (blue circles) and molecular (green diamonds) systems. The good agreement observed suggests that  $1/\Gamma$  is a suitable modification factor to the YH correction for MS diffusion coefficients. Hence, eq 16 can be rewritten as

$$\mathcal{D}_{\text{MS}}^{\infty} - \mathcal{D}_{\text{MS}}^{\text{MD}} = \alpha D^{\text{YH}} \approx \left( \frac{1}{\Gamma} \right) D^{\text{YH}} \quad (17)$$

In the rest of the manuscript, the last term ( $D^{\text{YH}}/\Gamma$ ) will be called the “Maxwell–Stefan Yeh–Hummer (MSYH)” correction ( $\mathcal{D}^{\text{MSYH}} = D^{\text{YH}}/\Gamma$ ). The results shown in Figure 4 suggest that describing the correction for MS as a function of only  $\Gamma$  seems to be sufficient; however, the possibility that other (still unknown) factors contribute to the correction cannot be ruled out. The applicability of  $\mathcal{D}^{\text{MSYH}}$  in multicomponent mixtures is not examined in this work.

By combining eqs 11 and 17, the finite-size correction to the Fick diffusion coefficient for a binary mixture can be calculated from

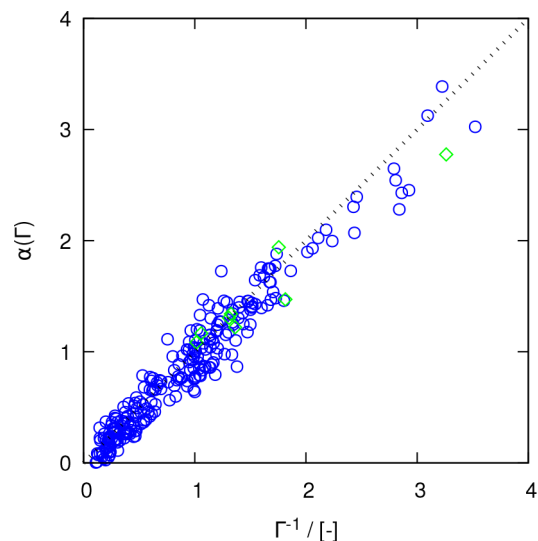


**Figure 4.** Modification factor to the YH correction ( $\alpha$ ) as a function of the thermodynamic factor ( $\Gamma$ ) for nonideal mixtures according to eq 16. Blue circles and green diamonds show the modification factors for the LJ and molecular systems, respectively. The thermodynamic factor for ideal mixtures equals 1. The dashed line indicates perfect agreement. Statistical uncertainties are listed in the Supporting Information.

$$\begin{aligned}
 D_{\text{Fick}}^{\infty} - D_{\text{Fick}}^{\text{MD}} &= \Gamma \mathcal{D}_{\text{MS}}^{\infty} - \Gamma \mathcal{D}_{\text{MS}}^{\text{MD}} = \Gamma (\mathcal{D}_{\text{MS}}^{\infty} - \mathcal{D}_{\text{MS}}^{\text{MD}}) \\
 &= \Gamma \left( \frac{1}{\Gamma} D^{\text{YH}} \right) = D^{\text{YH}} \quad (18)
 \end{aligned}$$

where  $D_{\text{Fick}}^{\infty}$  and  $D_{\text{Fick}}^{\text{MD}}$  are Fick diffusivities in infinite and finite-size systems, respectively. Interestingly, the same YH correction that is applied to self-diffusivities can mitigate the finite-size effects of Fick diffusion coefficients, regardless of the ideality or nonideality of the mixture.

In Figure 5, the correction for the finite-size effects of MS diffusion coefficients ( $\mathcal{D}_{\text{MS}}^{\infty} - \mathcal{D}_{\text{MS}}^{\text{MD}}$ ) are compared to the predicted MSYH correction ( $\mathcal{D}^{\text{MSYH}}$ ) for the studied LJ (Figure 5a) and molecular systems (Figure 5b). As expected from Figure 4, a rather good agreement can be seen for both sets. These results suggest that  $\mathcal{D}^{\text{MSYH}}$  works equally good for simple systems such as LJ systems and for nonspherical molecular systems with long-range electrostatic interactions. As proposed by Moulton et al.,<sup>69</sup> a minimum number of 250 molecules was used for all molecular systems. For a smaller number of particles, the shape and anisotropic structure of constituent molecules may play a role and affect the accuracy of the YH correction. Since no outlier is observed for the molecular systems in Figure 5b, the same criterion for the minimum number of molecules seems to be applicable to the MSYH correction.

While the proposed MSYH correction (see Figure 5) seems to perform fairly accurately, two important points should be noted. (1) The MSYH correction overpredicts the finite-size effects of MS diffusivities for LJ systems. This is consistent with the earlier observations for self-diffusivities (Figure 2a). The MSYH correction is based on the YH correction (Equation 17), so any overprediction of  $D^{\text{YH}}$  will affect  $\mathcal{D}^{\text{MSYH}}$ . To show the cause of this overprediction, the same comparison as in Figure 5, between the required corrections, is considered. However, instead of the analytic YH correction, the differences between the computed infinite and finite-size Darken diffusivities are

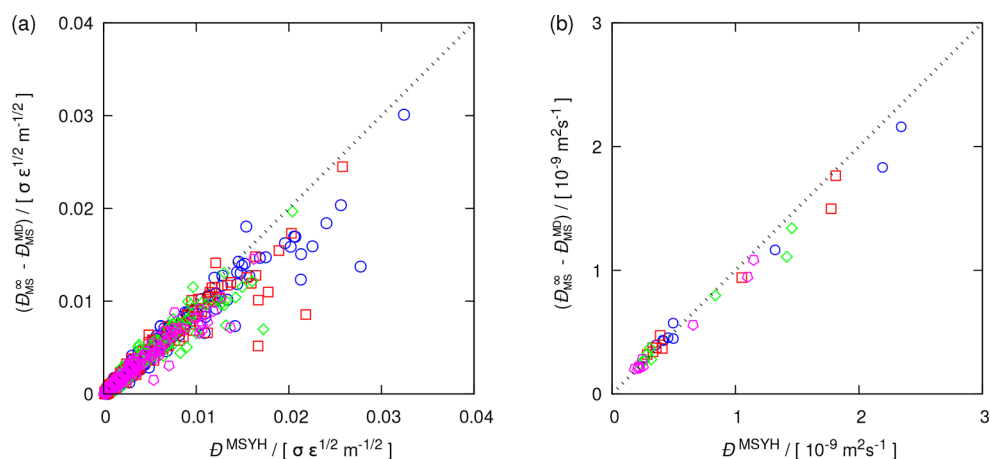


**Figure 5.** Correction needed for the MS diffusion coefficients versus the MSYH correction term ( $D^{\text{MSYH}}$ , eq 17) for (a) LJ and (b) molecular systems computed with 500 LJ particles/250 molecules (blue circles), 1000 LJ particles/500 molecules (red squares), 2000 LJ particles/1000 molecules (green diamonds), and 4000 LJ particles/2000 molecules (magenta pentagons). The dashed lines show perfect agreement. The statistical uncertainties are listed in the [Supporting Information](#).

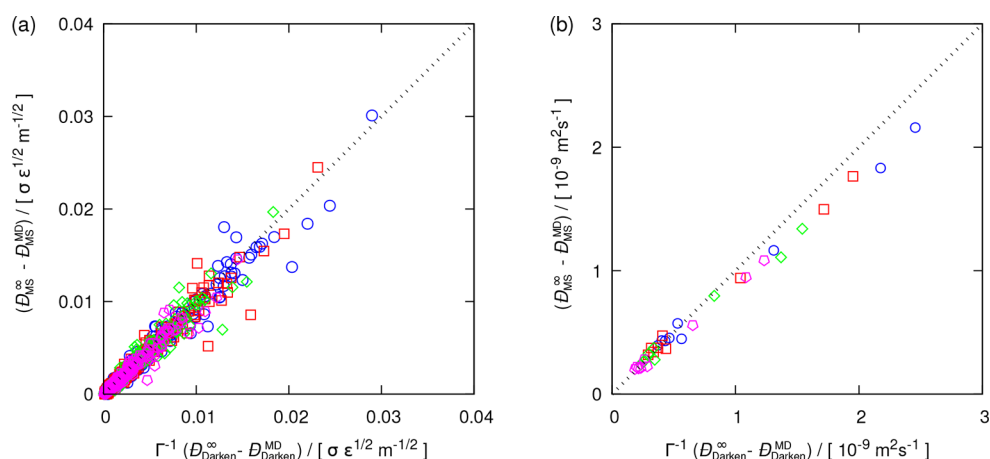


**Figure 6.** Correction needed for the MS diffusion coefficients versus the extrapolated Darken equation with the modification factor included ( $\Gamma^{-1}(D_{\text{Darken}}^{\infty} - D_{\text{Darken}}^{\text{MD}})$ ) for (a) LJ and (b) molecular systems computed with 500 LJ particles/250 molecules (blue circles), 1000 LJ particles/500 molecules (red squares), 2000 LJ particles/1000 molecules (green diamonds), and 4000 LJ particles/2000 molecules (magenta pentagons). The dashed lines show perfect agreement. The statistical uncertainties are listed in the [Supporting Information](#).

used (see [Figure 6](#)). For molecular mixtures, no difference is noticed. This is expected since the YH correction performs well according to [Figure 2b](#). Note that the overprediction observed in [Figures 2a](#) and [5a](#) is not present in [Figure 6a](#) and the data points are symmetrically distributed on both sides of the diagonal line. This indicates that the less accurate predictions by the YH correction resulted in the overpredictions shown in [Figure 5](#) and that the proposed modification of eq 17 does not introduce any systematic deviations. (2) The data points shown in [Figures 4–6](#) for MS diffusivities are more scattered compared to those of self-diffusion coefficients illustrated in [Figure 2](#). The cause can be the large statistical uncertainties of thermodynamic factors and finite-size MS diffusivities as well as the extrapolation of MS diffusion coefficients ( $D_{\text{MS}}$ ) to the thermodynamic limit (reported in the [Supporting Information](#)). These influences are expected to contribute to the scattering of the data in [Figures 4](#) and [5](#).

As the MSYH correction is related to the YH correction via the thermodynamic factor, three possible scenarios for studying the significance of the MSYH correction can be conceived: (1) In the case of  $\Gamma = 1$ , the behavior of the mixture is ideal. The

YH correction can directly be applied to self, MS, and Fick diffusivities. (2) For  $0 < \Gamma < 1$ , the constituent species of the mixture tend to self-associate and the cross-interactions are less pronounced. Since  $\Gamma$  is smaller than 1, the modification factor makes the MSYH correction larger than the YH correction. (3) For associating mixtures with thermodynamic factors larger than 1, the correction decreases to smaller values than the YH correction. For mixtures with very large thermodynamic factors, the finite-size correction becomes negligible and overlaps with the statistical uncertainty of the computed MS diffusion coefficient.

To show the importance of the MSYH correction for systems with  $0 < \Gamma < 1$ , we consider a mixture of methanol–carbon tetrachloride ( $x_{\text{methanol}} = 0.90$ ). This mixture has a small thermodynamic factor approximately equal to 0.18. Accordingly, the modification factor to the YH correction for MS diffusivities would be approximately 6 ( $\approx 1/0.18$ ). To investigate the magnitude of the finite-size effect, in [Figure 7](#), the Darken and MS diffusion coefficients of this mixture are shown for four system sizes. As expected, both the YH and MSYH corrections can accurately predict the finite-size

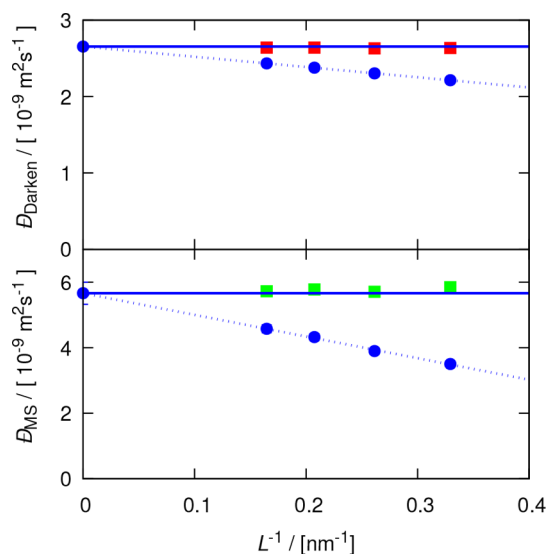


**Figure 7.** Binary Darken (Equation 10) and MS (Equation 8) diffusivities for a mixture of methanol–carbon tetrachloride ( $x_{\text{methanol}} = 0.9$ ) as a function of the simulation box ( $L$ ). Blue circles are the computed diffusion coefficients in MD simulations. Red and green squares are the corrected diffusivities according to the YH (Equation 2) and MSYH (eq 17) corrections, respectively. Dashed lines show extrapolation to the thermodynamic limit, and solid lines are the extrapolated values.

diffusivities. Whereas the finite-size effect for the self-diffusivities is at most 20% of the uncorrected value, the finite-size effect for MS diffusivities can be as large as 60% of the computed values in the current MD simulations. The contribution of the finite-size effect becomes even more pronounced for  $\Gamma \rightarrow 0$ , i.e., close to demixing. Therefore, considering the MSYH correction is particularly important for such systems.

## 5. CONCLUSION

Molecular dynamics is a powerful tool to predict binary diffusion coefficients of nonideal mixtures. Even with modern computers, the number of molecules used in a typical simulation is orders of magnitude lower than the thermodynamic limit; therefore, it is important to take into account finite-size effects when calculating diffusion coefficients. Yeh and Hummer have developed a correction term ( $D^{\text{YH}}$ ) to compensate for the finite-size effects of self-diffusion coefficients of pure fluids. This correction is a function of only the shear viscosity and the length of the simulation box. In this work, we verified the applicability of this correction to a wide range of nonideal binary mixtures. On the basis of the work of Yeh and Hummer, we present a Maxwell–Stefan YH correction,  $\mathcal{D}^{\text{MSYH}}$ , for finite-size effects of computed Maxwell–Stefan diffusion coefficients,  $\mathcal{D}^{\text{MSYH}} = D^{\text{YH}}/\Gamma$ , in which  $\Gamma$  is the thermodynamic factor. This correction is verified for a large set of Lennard–Jones systems as well as several molecular mixtures, and excellent predictions are obtained. For mixtures with a thermodynamic factor close to zero (i.e., close to demixing), this correction may become even larger than the computed finite-size Maxwell–Stefan diffusion coefficient. This highlights the importance of the finite-size corrections. In future work, a similar correction may be derived for multicomponent mixtures, in which the formulation of Maxwell–Stefan diffusivities is much more complex than those for binary mixtures.<sup>42,80</sup>

## ■ ASSOCIATED CONTENT

### Supporting Information

The Supporting Information is available free of charge on the ACS Publications website at DOI: 10.1021/acs.jctc.8b00170.

The force field parameters, for both Lennard–Jones (LJ) and molecular mixtures; a detailed description of all MD simulation results for different system sizes (PDF) Simulation results (diffusivities and viscosities) for all studied LJ and molecular systems (ZIP) LAMMPS code (ZIP)

## ■ AUTHOR INFORMATION

### Corresponding Author

\*E-mail: o.moultos@tudelft.nl.

### ORCID

Seyed Hossein Jamali: 0000-0002-4198-0901

Tim M. Becker: 0000-0002-6601-4320

André Bardow: 0000-0002-3831-0691

Thijs J. H. Vlugt: 0000-0003-3059-8712

Othonas A. Moultos: 0000-0001-7477-9684

### Funding

This work was sponsored by NWO Exacte Wetenschappen (Physical Sciences) for the use of supercomputer facilities, with financial support from the Nederlandse Organisatie voor Wetenschappelijk Onderzoek (Netherlands Organisation for Scientific Research, NWO). T.J.H.V. acknowledges NWO-CW (Chemical Sciences) for a VICI grant.

### Notes

The authors declare no competing financial interest.

## ■ NOMENCLATURE

$\alpha$ , constant coefficient (–);  $\mathbf{r}_{j,i}$ , position of molecule  $j$  of species  $i$  (m);  $\mathcal{D}^{\text{MSYH}}$ , Maxwell–Stefan Yeh–Hummer (MSYH) correction to finite-size MS diffusivity ( $\text{m}^2\cdot\text{s}^{-1}$ );  $\mathcal{D}_{\text{Darken}}$ , Maxwell–Stefan (MS) diffusivity in ideal mixtures computed from Darken equation (eq 10) ( $\text{m}^2\cdot\text{s}^{-1}$ );  $\mathcal{D}_{\text{MS}}$ , Maxwell–Stefan (MS) diffusivity ( $\text{m}^2\cdot\text{s}^{-1}$ );  $\mathcal{D}_{\text{MS}}^{\text{MD}}$ , Maxwell–Stefan (MS) diffusivity computed from MD simulations ( $\text{m}^2\cdot\text{s}^{-1}$ );  $\mathcal{D}_{\text{MS}}^{\infty}$ , Maxwell–Stefan (MS) diffusivity in the thermodynamic limit ( $\text{m}^2\cdot\text{s}^{-1}$ );  $\delta_{ij}$ , Kronecker delta (–);  $\epsilon_i$ , Lennard–Jones (LJ) energy parameter for species  $i$  (e);  $\eta$ , shear viscosity (Pa·s);  $\Gamma$ , thermodynamic factor (–);  $\gamma_i$ , activity coefficient of species  $i$  (–);  $\Lambda_{ij}$ , Onsager coefficient ( $\text{m}^2\cdot\text{s}^{-1}$ );  $\sigma_i$ , Lennard–Jones (LJ) size parameter for species  $i$  (Å);  $\xi$ , Constant value for the YH correction, 2.837297 for cubic simulation boxes (–);  $c_i$ , total number density ( $\text{m}^{-3}$ );  $CC_{ij}$ , displacement crosscorrelation function of species  $i$  and  $j$  ( $\text{m}^2\cdot\text{s}^{-1}$ );  $CC_{ij}^{\text{MD}}$ , finite-size displacement crosscorrelation function of species  $i$  and  $j$  computed from MD simulations ( $\text{m}^2\cdot\text{s}^{-1}$ );  $CC_{ij}^{\infty}$ , displacement crosscorrelation function of species  $i$  and  $j$  in the thermodynamic limit ( $\text{m}^2\cdot\text{s}^{-1}$ );  $D^{\text{YH}}$ , Yeh–Hummer (YH) correction to finite-size self-diffusivity ( $\text{m}^2\cdot\text{s}^{-1}$ );  $D_{\text{Fick}}$ , Fick diffusivity ( $\text{m}^2\cdot\text{s}^{-1}$ );  $D_{\text{Fick}}^{\text{MD}}$ , Fick diffusivity resulted from MD simulations ( $\text{m}^2\cdot\text{s}^{-1}$ );  $D_{\text{Fick}}^{\infty}$ , Fick diffusivity in the thermodynamic limit ( $\text{m}^2\cdot\text{s}^{-1}$ );  $D_{i,\text{self}}$ , self-diffusivity of species  $i$  ( $\text{m}^2\cdot\text{s}^{-1}$ );  $D_{i,\text{self}}^{\text{MD}}$ , self-diffusivity of species  $i$  computed from MD simulations ( $\text{m}^2\cdot\text{s}^{-1}$ );  $D_{i,\text{self}}^{\infty}$ , self-diffusivity of species  $i$  in the thermodynamic limit ( $\text{m}^2\cdot\text{s}^{-1}$ );  $G_{ij}$ , Kirkwood–Buff coefficient between species  $i$  and  $j$  ( $\text{m}^3$ );  $g_{ij}$ , radial distribution function (RDF) between species  $i$  and  $j$  (–);  $k_B$ , Boltzmann constant ( $= 1.38065 \times 10^{23} \text{ J}\cdot\text{K}^{-1}$ );  $k_{ij}$ , an adjustable parameter for the Lorentz–Berthelot mixing rules



(–);  $L$ , side length of the cubic simulation box (m);  $M_i$ , molar mass of species  $i$  ( $\text{kg}\cdot\text{mol}^{-1}$ );  $m_i$ , mass of a Lennard–Jones (LJ) particle (m);  $N$ , total number of molecules (–);  $N_i$ , number of molecules of species  $i$  (–);  $p$ , hydrostatic pressure (Pa);  $P_{\alpha\beta}$ , off-diagonal stress tensor components (Pa);  $T$ , temperature (K);  $t$ , time (s);  $V$ , volume of the simulation box ( $\text{m}^3$ );  $x_i$ , mole fraction of species  $i$  (–)

## REFERENCES

- (1) Kohl, A. L.; Nielsen, R. *Gas Purification*, 5th ed.; Gulf Professional Publishing: Houston, 1997.
- (2) Lyons, W.; Plisga, G. J.; Lorenz, M. *Standard Handbook of Petroleum and Natural Gas Engineering*, 3rd ed.; Gulf Professional Publishing: Waltham, 2015.
- (3) Economou, I.; Krokidas, P.; Michalis, V.; Moulto, O.; Tsimpanogiannis, I.; Vergadou, N. *The Water-Food-Energy Nexus: Processes, Technologies, and Challenges*; CRC Press: Boca Raton, 2017; Chapter 13, pp 633–660.
- (4) Economou, I. G.; de Hemptinne, J.-C.; Dohrn, R.; Hendriks, E.; Keskinen, K.; Baudouin, O. Industrial Use of Thermodynamics Workshop: Round Table Discussion on 8 July 2014. *Chem. Eng. Res. Des.* **2014**, *92*, 2795–2796.
- (5) Liu, X.; Vlugt, T. J. H.; Bardow, A. Maxwell-Stefan Diffusivities in Binary Mixtures of Ionic Liquids with Dimethyl Sulfoxide (DMSO) and  $\text{H}_2\text{O}$ . *J. Phys. Chem. B* **2011**, *115*, 8506–8517.
- (6) Liu, X.; Bardow, A.; Vlugt, T. J. H. Multicomponent Maxwell-Stefan Diffusivities at Infinite Dilution. *Ind. Eng. Chem. Res.* **2011**, *50*, 4776–4782.
- (7) Liu, X.; Schnell, S. K.; Simon, J.-M.; Bedeaux, D.; Kjelstrup, S.; Bardow, A.; Vlugt, T. J. H. Fick Diffusion Coefficients of Liquid Mixtures Directly Obtained From Equilibrium Molecular Dynamics. *J. Phys. Chem. B* **2011**, *115*, 12921–12929.
- (8) Liu, X.; Martín-Calvo, A.; McGarrity, E.; Schnell, S. K.; Calero, S.; Simon, J.-M.; Bedeaux, D.; Kjelstrup, S.; Bardow, A.; Vlugt, T. J. H. Fick Diffusion Coefficients in Ternary Liquid Systems from Equilibrium Molecular Dynamics Simulations. *Ind. Eng. Chem. Res.* **2012**, *51*, 10247–10258.
- (9) Liu, X.; Schnell, S. K.; Simon, J.-M.; Krüger, P.; Bedeaux, D.; Kjelstrup, S.; Bardow, A.; Vlugt, T. J. H. Diffusion Coefficients from Molecular Dynamics Simulations in Binary and Ternary Mixtures. *Int. J. Thermophys.* **2013**, *34*, 1169–1196.
- (10) Pappaert, K.; Biesemans, J.; Clicq, D.; Vankrunkelsven, S.; Desmet, G. Measurements of Diffusion Coefficients in 1-D Micro- and Nanochannels Using Shear-Driven Flows. *Lab Chip* **2005**, *5*, 1104–1110.
- (11) Peters, C.; Wolff, L.; Vlugt, T. J. H.; Bardow, A. In *Experimental Thermodynamics Volume X*; Bedeaux, D., Kjelstrup, S., Sengers, J., Eds.; Royal Society of Chemistry: Cropton, 2015; Chapter 5, pp 78–104.
- (12) Bouchaudy, A.; Loussert, C.; Salmon, J.-B. Steady Microfluidic Measurements of Mutual Diffusion Coefficients of Liquid Binary Mixtures. *AIChE J.* **2018**, *64*, 358–366.
- (13) Bardow, A.; Marquardt, W.; Göke, V.; Koss, H.-J.; Lucas, K. Model-Based Measurement of Diffusion Using Raman Spectroscopy. *AIChE J.* **2003**, *49*, 323–334.
- (14) Bardow, A.; Göke, V.; Koß, H.-J.; Marquardt, W. Ternary diffusivities by model-based analysis of Raman spectroscopy measurements. *AIChE J.* **2006**, *52*, 4004–4015.
- (15) Wolff, L.; Koß, H.-J.; Bardow, A. The Optimal Diffusion Experiment. *Chem. Eng. Sci.* **2016**, *152*, 392–402.
- (16) Peters, C.; Wolff, L.; Haase, S.; Thien, J.; Brands, T.; Koß, H.-J.; Bardow, A. Multicomponent Diffusion Coefficients from Microfluidics Using Raman Microspectroscopy. *Lab Chip* **2017**, *17*, 2768–2776.
- (17) Woolf, L. A.; Mills, R.; Leaist, D.; Erkey, C.; Akgerman, A.; Eastale, A. J.; Miller, D.; Albright, J. G.; Li, S. F. Y.; Wakeham, W. In *Measurement of the transport properties of fluids*; Wakeham, W. A., Nagashima, A., Sengers, J. V., Eds.; Blackwell Scientific Publications: Boston, 1991; Chapter 9, pp 228–320.
- (18) Edward, J. T. Molecular Volumes and the Stokes-Einstein Equation. *J. Chem. Educ.* **1970**, *47*, 261.
- (19) Fuller, E. N.; Schettler, P. D.; Giddings, J. C. New Method for Prediction of Binary Gas-Phase Diffusion Coefficient. *Ind. Eng. Chem.* **1966**, *58*, 18–27.
- (20) Wilke, C. R.; Chang, P. Correlation of Diffusion Coefficients in Dilute Solutions. *AIChE J.* **1955**, *1*, 264–270.
- (21) Sandler, S. I.; Mason, E. a. Kinetic-Theory Deviations from Blanc's Law of Ion Mobilities. *J. Chem. Phys.* **1968**, *48*, 2873–2875.
- (22) Chapman, S.; Cowling, T. G. *The Mathematical Theory of Non-Uniform Gases*, 3rd ed.; Cambridge University Press: Cambridge, 1970.
- (23) Tyrrell, H. J. V. *Diffusion in Liquids: A Theoretical and Experimental Study*; Butterworth-Heinemann: Cambridge, 1984.
- (24) Dymond, J. H. Hard-Sphere Theories of Transport Properties. *Chem. Soc. Rev.* **1985**, *14*, 317.
- (25) Poling, B. E.; Prausnitz, J. M.; O'Connell, J. P. *The Properties of Gases and Liquids*, 5th ed.; McGraw-Hill: New York, 2001.
- (26) Bird, R. B. *Transport Phenomena*, 2nd ed.; John Wiley & Sons: New York, 2007.
- (27) Cussler, E. L. *Diffusion: Mass Transfer in Fluid Systems*, 3rd ed.; Cambridge University Press: Cambridge, 2009.
- (28) Evans, D. J.; Morriss, G. *Statistical Mechanics of Nonequilibrium Liquids*, 2nd ed.; Cambridge University Press: Cambridge, 2008.
- (29) Alder, B. J.; Gass, D. M.; Wainwright, T. E. Studies in Molecular Dynamics. VIII. The Transport Coefficients for a Hard-Sphere Fluid. *J. Chem. Phys.* **1970**, *53*, 3813–3826.
- (30) van de Ven-Lucassen, I. M. J. J.; Kemmere, M. F.; Kerkhof, P. J. A. M. Complications in the use of the Taylor dispersion method for ternary diffusion measurements: Methanol + acetone + water mixtures. *J. Solution Chem.* **1997**, *26*, 1145–1167.
- (31) van de Ven-Lucassen, I. M. J. J.; Vlugt, T. J. H.; van der Zanden, A. J. J.; Kerkhof, P. J. A. M. Molecular Dynamics Simulation of Self-Diffusion and Maxwell-Stefan Diffusion Coefficients in Liquid Mixtures of Methanol and Water. *Mol. Simul.* **1999**, *23*, 79–94.
- (32) Krishna, R.; van Baten, J. M. The Darken Relation for Multicomponent Diffusion in Liquid Mixtures of Linear Alkanes: An Investigation Using Molecular Dynamics (MD) Simulations. *Ind. Eng. Chem. Res.* **2005**, *44*, 6939–6947.
- (33) Krishna, R.; van Baten, J. M. MD Simulations of Diffusivities in Methanol-n-hexane Mixtures Near the Liquid-liquid Phase Splitting Region. *Chem. Eng. Technol.* **2006**, *29*, 516–519.
- (34) Krishna, R.; van Baten, J. M. Validating the Darken Relation for Diffusivities in Fluid Mixtures of Varying Densities by Use of MD Simulations. *Chem. Eng. Technol.* **2006**, *29*, 761–765.
- (35) Parez, S.; Guevara-Carrion, G.; Hasse, H.; Vrabec, J. Mutual Diffusion in the Ternary Mixture of Water + Methanol + Ethanol and its Binary Subsystems. *Phys. Chem. Chem. Phys.* **2013**, *15*, 3985.
- (36) Moulto, O. A.; Tsimpanogiannis, I. N.; Panagiotopoulos, A. Z.; Economou, I. G. Atomistic Molecular Dynamics Simulations of  $\text{CO}_2$  Diffusivity  $\text{H}_2\text{O}$  for a Wide Range of Temperatures and Pressures. *J. Phys. Chem. B* **2014**, *118*, 5532–5541.
- (37) Guevara-Carrion, G.; Gaponenko, Y.; Janzen, T.; Vrabec, J.; Shevtsova, V. Diffusion in Multicomponent Liquids: From Microscopic to Macroscopic Scales. *J. Phys. Chem. B* **2016**, *120*, 12193–12210.
- (38) Guevara-Carrion, G.; Janzen, T.; Muñoz-Muñoz, Y. M.; Vrabec, J. In *High Performance Computing in Science and Engineering '16*; Nagel, W. E., Kröner, D. H., Resch, M. M., Eds.; Springer International Publishing: Cham, 2016; pp 613–634.
- (39) Moulto, O. A.; Tsimpanogiannis, I. N.; Panagiotopoulos, A. Z.; Trusler, J. P. M.; Economou, I. G. Atomistic Molecular Dynamics Simulations of Carbon Dioxide Diffusivity in n-Hexane, n-Decane, n-Hexadecane, Cyclohexane, and Squalane. *J. Phys. Chem. B* **2016**, *120*, 12890–12900.
- (40) Jiang, H.; Moulto, O. A.; Economou, I. G.; Panagiotopoulos, A. Z. Hydrogen-Bonding Polarizable Intermolecular Potential Model for Water. *J. Phys. Chem. B* **2016**, *120*, 12358–12370.

- (41) Jiang, H.; Moulto, O. A.; Economou, I. G.; Panagiotopoulos, A. Z. Gaussian-Charge Polarizable and Nonpolarizable Models for CO<sub>2</sub>. *J. Phys. Chem. B* **2016**, *120*, 984–994.
- (42) Krishna, R.; Wesselingh, J. The Maxwell-Stefan approach to mass transfer. *Chem. Eng. Sci.* **1997**, *52*, 861–911.
- (43) Taylor, R.; Krishna, R. *Multicomponent Mass Transfer*; John Wiley & Sons: New York, 1993.
- (44) Wesselingh, J. A.; Krishna, R. *Mass Transfer in Multicomponent Mixtures*; VSSD: Delft, 2006.
- (45) Krishna, R.; van Baten, J. An Investigation of the Characteristics of Maxwell-Stefan Diffusivities of Binary Mixtures in Silica Nanopores. *Chem. Eng. Sci.* **2009**, *64*, 870–882.
- (46) Krishna, R.; van Baten, J. Unified Maxwell-Stefan Description of Binary Mixture Diffusion in Micro- and Meso-Porous Materials. *Chem. Eng. Sci.* **2009**, *64*, 3159–3178.
- (47) Krishna, R.; van Baten, J. M. Highlighting Pitfalls in the Maxwell-Stefan Modeling of Water-Alcohol Mixture Permeation Across Pervaporation Membranes. *J. Membr. Sci.* **2010**, *360*, 476–482.
- (48) Krishna, R. The Maxwell-Stefan Description of Mixture Diffusion in Nanoporous Crystalline Materials. *Microporous Mesoporous Mater.* **2014**, *185*, 30–50.
- (49) Han, K. N.; Bernardi, S.; Wang, L.; Searles, D. J. Water Diffusion in Zeolite Membranes: Molecular Dynamics Studies on Effects of Water Loading and Thermostat. *J. Membr. Sci.* **2015**, *495*, 322–333.
- (50) Krishna, R. Using the Maxwell-Stefan Formulation for Highlighting the Influence of Interspecies (1–2) Friction on Binary Mixture Permeation Across Microporous and Polymeric Membranes. *J. Membr. Sci.* **2017**, *540*, 261–276.
- (51) Schoen, M.; Hoheisel, C. The Mutual Diffusion Coefficient  $D_{12}$  in Binary Liquid Model Mixtures. Molecular Dynamics Calculations Based on Lennard-Jones (12–6) Potentials. *Mol. Phys.* **1984**, *52*, 33–56.
- (52) Schoen, M.; Hoheisel, C. The Mutual Diffusion Coefficient  $D_{12}$  in Liquid Model Mixtures A Molecular Dynamics Study Based on Lennard-Jones (12–6) Potentials. *Mol. Phys.* **1984**, *52*, 1029–1042.
- (53) Weingärtner, H. The Microscopic Basis of Self Diffusion - Mutual Diffusion Relationships in Binary Liquid Mixtures. *Berichte der Bunsengesellschaft für Phys. Chemie* **1990**, *94*, 358–364.
- (54) Liu, X.; Vlugt, T. J. H.; Bardow, A. Predictive Darken Equation for Maxwell-Stefan Diffusivities in Multicomponent Mixtures. *Ind. Eng. Chem. Res.* **2011**, *50*, 10350–10358.
- (55) Liu, X.; Vlugt, T. J. H.; Bardow, A. Maxwell-Stefan Diffusivities in Liquid Mixtures: Using Molecular Dynamics for Testing Model Predictions. *Fluid Phase Equilib.* **2011**, *301*, 110–117.
- (56) D'Agostino, C.; Stephens, J.; Parkinson, J.; Mantle, M.; Gladden, L.; Moggridge, G. Prediction of the Mutual Diffusivity in Acetone-Chloroform Liquid Mixtures from the Tracer Diffusion Coefficients. *Chem. Eng. Sci.* **2013**, *95*, 43–47.
- (57) Guevara-Carrion, G.; Janzen, T.; Muñoz-Muñoz, Y. M.; Vrabec, J. Mutual Diffusion of Binary Liquid Mixtures Containing Methanol, Ethanol, Acetone, Benzene, Cyclohexane, Toluene, and Carbon Tetrachloride. *J. Chem. Phys.* **2016**, *144*, 124501.
- (58) Allie-Ebrahim, T.; Zhu, Q.; Bräuer, P.; Moggridge, G. D.; D'Agostino, C. Maxwell-Stefan diffusion Coefficient Estimation for Ternary Systems: An Ideal Ternary Alcohol system. *Phys. Chem. Chem. Phys.* **2017**, *19*, 16071–16077.
- (59) Fisher, M.; Barber, M. Scaling Theory for Finite-Size Effects in the Critical Region. *Phys. Rev. Lett.* **1972**, *28*, 1516–1519.
- (60) Hilfer, R.; Wilding, N. B. Are Critical Finite-Size Scaling Functions Calculable from Knowledge of an Appropriate Critical Exponent? *J. Phys. A: Math. Gen.* **1995**, *28*, L281.
- (61) Das, S. K.; Fisher, M. E.; Sengers, J. V.; Horbach, J.; Binder, K. Critical Dynamics in a Binary Fluid: Simulations and Finite-Size Scaling. *Phys. Rev. Lett.* **2006**, *97*, 025702.
- (62) Binder, K. Theory of First-Order Phase Transitions. *Rep. Prog. Phys.* **1987**, *50*, 783–859.
- (63) Wilding, N. B. Critical-Point and Coexistence-Curve Properties of the Lennard-Jones Fluid: A Finite-Size Scaling Study. *Phys. Rev. E: Stat. Phys., Plasmas, Fluids, Relat. Interdiscip. Top.* **1995**, *52*, 602–611.
- (64) Bruce, A. D.; Wilding, N. B. Critical-Point Finite-Size Scaling in the Microcanonical Ensemble. *Phys. Rev. E: Stat. Phys., Plasmas, Fluids, Relat. Interdiscip. Top.* **1999**, *60*, 3748–3760.
- (65) Dünweg, B.; Kremer, K. Molecular Dynamics Simulation of a Polymer Chain in Solution. *J. Chem. Phys.* **1993**, *99*, 6983–6997.
- (66) Yeh, I.-C.; Hummer, G. System-Size Dependence of Diffusion Coefficients and Viscosities from Molecular Dynamics Simulations with Periodic Boundary Conditions. *J. Phys. Chem. B* **2004**, *108*, 15873–15879.
- (67) Heyes, D. M.; Cass, M. J.; Powles, J. G.; Evans, W. A. B. Self-Diffusion Coefficient of the Hard-Sphere Fluid: System Size Dependence and Empirical Correlations. *J. Phys. Chem. B* **2007**, *111*, 1455–1464.
- (68) Moulto, O. A.; Orozco, G. A.; Tsimpanogiannis, I. N.; Panagiotopoulos, A. Z.; Economou, I. G. Atomistic Molecular Dynamics Simulations of H<sub>2</sub>O Diffusivity in Liquid and Supercritical CO<sub>2</sub>. *Mol. Phys.* **2015**, *113*, 2805–2814.
- (69) Moulto, O. A.; Zhang, Y.; Tsimpanogiannis, I. N.; Economou, I. G.; Maginn, E. J. System-Size Corrections for Self-Diffusion Coefficients Calculated from Molecular Dynamics Simulations: The Case of CO<sub>2</sub>, n-alkanes, and Poly(Ethylene Glycol) Dimethyl Ethers. *J. Chem. Phys.* **2016**, *145*, 074109.
- (70) Wheeler, D. R.; Rowley, R. L. Shear Viscosity of Polar Liquid Mixtures via Non-equilibrium Molecular Dynamics: Water, Methanol, and Acetone. *Mol. Phys.* **1998**, *94*, 555–564.
- (71) Arya, G.; Maginn, E. J.; Chang, H.-C. Efficient Viscosity Estimation from Molecular Dynamics Simulation via Momentum Impulse Relaxation. *J. Chem. Phys.* **2000**, *113*, 2079.
- (72) Müller-Plathe, F. Reversing the Perturbation in Nonequilibrium Molecular Dynamics: An Easy Way to Calculate the Shear Viscosity of Fluids. *Phys. Rev. E: Stat. Phys., Plasmas, Fluids, Relat. Interdiscip. Top.* **1999**, *59*, 4894–4898.
- (73) Müller-Plathe, F. A Simple Nonequilibrium Molecular Dynamics Method for Calculating the Thermal Conductivity. *J. Chem. Phys.* **1997**, *106*, 6082–6085.
- (74) Yang, H.; Zhang, J.; Müller-Plathe, F.; Yang, Y. A Reverse Nonequilibrium Molecular Dynamics Method for Calculating the Mutual Diffusion Coefficient for Binary Fluids. *Chem. Eng. Sci.* **2015**, *130*, 1–7.
- (75) Frenkel, D.; Smit, B. *Understanding Molecular Simulation: From Algorithms to Applications*, 2nd ed.; Academic Press: London, 2002.
- (76) Song, Y.; Dai, L. L. The Shear Viscosities of Common Water Models by Non-Equilibrium Molecular Dynamics Simulations. *Mol. Simul.* **2010**, *36*, 560–567.
- (77) Allen, M. P.; Tildesley, D. J. *Computer Simulation of Liquids*, 2nd ed.; Oxford University Press: Croydon, 2017.
- (78) Zwanzig, R. Time-Correlation Functions and Transport Coefficients in Statistical Mechanics. *Annu. Rev. Phys. Chem.* **1965**, *16*, 67–102.
- (79) Kooijman, H. A.; Taylor, R. Estimation of diffusion coefficients in multicomponent liquid systems. *Ind. Eng. Chem. Res.* **1991**, *30*, 1217–1222.
- (80) Krishna, R.; van Baten, J. M. Describing Diffusion in Fluid Mixtures at Elevated Pressures by Combining the Maxwell-Stefan Formulation with an Equation of State. *Chem. Eng. Sci.* **2016**, *153*, 174–187.
- (81) Guazzelli, E.; Morris, J. F. *A Physical Introduction to Suspension Dynamics*; Cambridge University Press: Cambridge, 2012.
- (82) Botan, A.; Marry, V.; Rotenberg, B. Diffusion in Bulk Liquids: Finite-Size Effects in Anisotropic Systems. *Mol. Phys.* **2015**, *113*, 2674–2679.
- (83) Vögele, M.; Hummer, G. Divergent Diffusion Coefficients in Simulations of Fluids and Lipid Membranes. *J. Phys. Chem. B* **2016**, *120*, 8722–8732.
- (84) Yang, X.; Zhang, H.; Li, L.; Ji, X. Corrections of the Periodic Boundary Conditions with Rectangular Simulation Boxes on the Diffusion Coefficient, General Aspects. *Mol. Simul.* **2017**, *43*, 1423–1429.

- (85) Simonnin, P.; Noetinger, B.; Nieto-Draghi, C.; Marry, V.; Rotenberg, B. Diffusion under Confinement: Hydrodynamic Finite-Size Effects in Simulation. *J. Chem. Theory Comput.* **2017**, *13*, 2881–2889.
- (86) Mondello, M.; Grest, G. S. Viscosity Calculations of n-Alkanes by Equilibrium Molecular Dynamics. *J. Chem. Phys.* **1997**, *106*, 9327.
- (87) Tenney, C. M.; Maginn, E. J. Limitations and Recommendations for the Calculation of Shear Viscosity Using Reverse Nonequilibrium Molecular Dynamics. *J. Chem. Phys.* **2010**, *132*, 014103.
- (88) Heyes, D. M. Pressure Tensor of Partial-Charge and Point-Dipole Lattices with Bulk and Surface Geometries. *Phys. Rev. B: Condens. Matter Mater. Phys.* **1994**, *49*, 755–764.
- (89) Thompson, A. P.; Plimpton, S. J.; Mattson, W. General Formulation of Pressure and Stress Tensor for Arbitrary Many-Body Interaction Potentials Under periodic Boundary Conditions. *J. Chem. Phys.* **2009**, *131*, 154107.
- (90) Zhou, Y.; Miller, G. H. Green–Kubo Formulas for Mutual Diffusion Coefficients in Multicomponent Systems. *J. Phys. Chem.* **1996**, *100*, 5516–5524.
- (91) Ben-Naim, A. *Molecular Theory of Solutions*; Oxford University Press: Oxford, 2006.
- (92) Krüger, P.; Schnell, S. K.; Bedeaux, D.; Kjelstrup, S.; Vlugt, T. J. H.; Simon, J.-M. Kirkwood-Buff Integrals for Finite Volumes. *J. Phys. Chem. Lett.* **2013**, *4*, 235–238.
- (93) Balaji, S. P.; Schnell, S. K.; McGarrity, E. S.; Vlugt, T. J. H. A Direct Method for Calculating Thermodynamic Factors for Liquid Mixtures Using the Permuted Widom Test Particle Insertion Method. *Mol. Phys.* **2013**, *111*, 287–296.
- (94) Balaji, S. P.; Schnell, S. K.; Vlugt, T. J. H. Calculating Thermodynamic Factors of Ternary and Multicomponent Mixtures Using the Permuted Widom Test Particle insertion Method. *Theor. Chem. Acc.* **2013**, *132*, 1333.
- (95) Dawass, N.; Krüger, P.; Schnell, S. K.; Bedeaux, D.; Kjelstrup, S.; Simon, J. M.; Vlugt, T. J. H. Finite-Size Effects of Kirkwood-Buff Integrals from Molecular Simulations. *Mol. Simul.* **2018**, *44*, 599–612.
- (96) Ganguly, P.; van der Veegt, N. F. A. Convergence of Sampling Kirkwood-Buff Integrals of Aqueous Solutions with Molecular Dynamics Simulations. *J. Chem. Theory Comput.* **2013**, *9*, 1347–1355.
- (97) Milzetti, J.; Nayar, D.; van der Veegt, N. F. A. Convergence of Kirkwood-Buff Integrals of Ideal and Non-Ideal Aqueous Solutions Using Molecular Dynamics Simulations. *J. Phys. Chem. B* **2018**, DOI: [10.1021/acs.jpcc.7b11831](https://doi.org/10.1021/acs.jpcc.7b11831).
- (98) Plimpton, S. Fast Parallel Algorithms for Short-Range Molecular Dynamics. *J. Comput. Phys.* **1995**, *117*, 1–19.
- (99) Martínez, L.; Andrade, R.; Birgin, E. G.; Martínez, J. M. PACKMOL: A Package for Building Initial Configurations for Molecular Dynamics Simulations. *J. Comput. Chem.* **2009**, *30*, 2157–2164.
- (100) Humphrey, W.; Dalke, A.; Schulten, K. VMD: Visual Molecular Dynamics. *J. Mol. Graphics* **1996**, *14*, 33–38.
- (101) Berendsen, H. J. C.; Grigera, J. R.; Straatsma, T. P. The Missing Term in Effective Pair Potentials. *J. Phys. Chem.* **1987**, *91*, 6269–6271.
- (102) Tummala, N. R.; Striolo, A. Hydrogen-Bond Dynamics for Water Confined in Carbon Tetrachloride-Acetone Mixtures. *J. Phys. Chem. B* **2008**, *112*, 10675–10683.
- (103) Chen, B.; Potoff, J. J.; Siepmann, J. I. Monte Carlo Calculations for Alcohols and Their Mixtures with Alkanes. Transferable Potentials for Phase Equilibria. 5. United-Atom Description of Primary, Secondary, and Tertiary Alcohols. *J. Phys. Chem. B* **2001**, *105*, 3093–3104.
- (104) Stubbs, J. M.; Potoff, J. J.; Siepmann, J. I. Transferable Potentials for Phase Equilibria. 6. United-Atom Description for Ethers, Glycols, Ketones, and Aldehydes. *J. Phys. Chem. B* **2004**, *108*, 17596–17605.
- (105) Wick, C. D.; Stubbs, J. M.; Rai, N.; Siepmann, J. I. Transferable Potentials for Phase Equilibria. 7. Primary, Secondary, and Tertiary Amines, Nitroalkanes and Nitrobenzene, Nitriles, Amides, Pyridine, and Pyrimidine. *J. Phys. Chem. B* **2005**, *109*, 18974–18982.
- (106) Martin, M. G.; Siepmann, J. I. Transferable Potentials for Phase Equilibria. 1. United-Atom Description of n-Alkanes. *J. Phys. Chem. B* **1998**, *102*, 2569–2577.
- (107) Guevara-Carrion, G.; Vrabec, J.; Hasse, H. Prediction of Self-Diffusion Coefficient and Shear Viscosity of Water and its Binary Mixtures with Methanol and Ethanol by Molecular Simulation. *J. Chem. Phys.* **2011**, *134*, 074508.
- (108) Michalis, V. K.; Moulton, O. A.; Tsimpanogiannis, I. N.; Economou, I. G. Molecular Dynamics Simulations of the Diffusion Coefficients of Light n-Alkanes in Water over a Wide Range of Temperature and Pressure. *Fluid Phase Equilib.* **2016**, *407*, 236–242.
- (109) Moulton, O. A.; Tsimpanogiannis, I. N.; Panagiotopoulos, A. Z.; Economou, I. G. Self-Diffusion Coefficients of the Binary (H<sub>2</sub>O + CO<sub>2</sub>) Mixture at High Temperatures and Pressures. *J. Chem. Thermodyn.* **2016**, *93*, 424–429.
- (110) Dubbeldam, D.; Ford, D. C.; Ellis, D. E.; Snurr, R. Q. A New Perspective on the Order-n Algorithm for Computing Correlation Functions. *Mol. Simul.* **2009**, *35*, 1084–1097.